



INTERNATIONAL ATOMIC ENERGY AGENCY
UNITED NATIONS EDUCATIONAL, SCIENTIFIC AND CULTURAL ORGANIZATION



INTERNATIONAL CENTRE FOR THEORETICAL PHYSICS

34100 TRIESTE (ITALY) - P.O.B. 550 - MIRAMARE - STRADA COSTIERA 11 - TELEPHONE: 2240-1
CABLE: CENTRATOM - TELEX 460392-1

SMR.379/39

COURSE ON BASIC TELECOMMUNICATIONS SCIENCE

9 January - 3 February 1989

OPTICAL FIBRES

W.A. Gambling

Department of Electronics and Information Engineering
University of Southampton
Southampton
SO9 5NH
U.K.

These notes are intended for internal distribution only.

OPTICAL FIBRES1. Introduction

The structure of optical fibre transmission lines takes the very simple [Suematsu & Iga 1982] form of a cylindrical glass core of refractive index n_1 surrounded by a cladding glass of refractive index n_2 where $n_2 < n_1$. Normally most of the propagating energy is contained in the core but there is always a radially-decaying evanescent field in the cladding, which may extend over several wavelengths in the case of single-mode fibres. Both core and cladding materials must therefore have very low absorption and scattering losses.

As with waveguides, when the transverse dimensions of the guiding structure, in this case the core, are comparable with a wavelength then only a single mode can be supported, whereas for larger core diameters multimode operation prevails. Normally the wavelength of operation is in the region of $1\mu\text{m}$, corresponding to a frequency of 300,000GHz, so that single-mode fibres have a core diameter of 1 to $10\mu\text{m}$ while multimode fibres have standardised core diameters of between 50 and $60\mu\text{m}$. For practical convenience the outer diameter of telecommunication fibres is made $125\mu\text{m}$ in both cases. In step-index fibres the refractive indices are constant in both core and cladding, whereas in (ideal) graded-index fibres the refractive index is a maximum n_1 at the core centre but falls monotonically to that of the cladding n_2 at the core boundary. With fibres designed for long-distance transmission $(n_1 - n_2) \leq n_1 \approx 1.5$ and the relative refractive-index $\Delta = (n_1 - n_2)/n_1$ is about 1%.

2. Extremely large bandwidths of up to 1GHzkm for graded-index multimode fibres and 100 GHzkm for single-mode fibres, ~20MHzkm for coaxial cable.
3. Small size, low weight and high degree of flexibility.
4. Freedom from electromagnetic interference and earth-loop problems.
5. Fabricated from relatively abundant materials (silica, phosphorus, germanium, boron).
6. Zero cross-talk between closely-spaced lines.
7. Larger Young's modulus and resistance to crushing than copper.

Disadvantages

1. Glass is brittle and therefore breaks when the elastic limit is exceeded.
2. Long-term (20 years) mechanical stability under strain is unknown.
3. Demountable connectors and other, similar, components are expensive.

The properties of the principal types of optical fibre waveguide are summarised in Table 1.

Optical fibres can have a wide variety of applications and can be made from a range of optically "transparent" materials. However, the most important fibres at the present time are those used in telecommunications and most attention, in the first part of this chapter, will therefore be devoted to them, although the general principles apply to all types of fibre. The principal component of such fibres is silica, which can be produced in very pure form (only a few parts of impurity in 10^9 parts of silica).

The glassy form [Rawson 1967] of pure SiO_2 has an extremely low transmission loss in the optical and near-infra-red regions of the spectrum and can be drawn into long lengths with a high degree of precision. Silica, unfortunately, has the low refractive index of 1.45 and, when used as the core of a fibre, there are comparatively few compatible materials which have a sufficiently low refractive index to act as cladding. Possibilities are silica admixed with a small proportion of boron or fluorine and certain plastics such as silicone rubber. Conversely the index of silica can be raised by adding such oxides as P_2O_5 , GeO_2 or TiO_2 .

Telecommunication fibres are generally prepared from a preform which is drawn down into a fibre which can be many (10-20) kilometres in length. The preform may contain three regions: a central core of fibre core material (e.g. germanosilicate glass); a surrounding layer of cladding glass (e.g. phosphosilicate glass); and an outer layer, or substrate, of commercial silica tubing. In the resulting fibre only the core and cladding

TABLE 1
PROPERTIES OF OPTICAL FIBRES

Type of Fibre	Core diameter (μm)	Materials	Transmission loss (dB/km)				BxL product
			0.85 μm	1.05 μm	1.3 μm	1.5 μm	
Single-mode	1-10	Core : silica based glass Cladding : silica based glass	2	1	0.38	0.15	50-100
		Core : silica based glass Cladding : silica based glass	2	1	0.5	0.15	0.005 to 0.02
	50-200	Core : silica based glass Cladding : plastic	2.5	1.5	high		
		Core : multi-component glass Cladding : multi-component glass	3.4	6	high		
Multi-mode	50-60	Silica glass	2	1	0.5	0.2	1
		Multicomponent glass	3.5	10	high		0.4

5

contribute to optical propagation and they must be of extremely high purity. There are several different methods of preform fabrication which are based on various forms of chemical vapour deposition [Gambling, Hartog & Ragdale 1981].

2. Transmission Loss of Optical Fibres

The factors contributing to loss in an optical fibre transmission line include absorption, scattering due to inhomogeneities in the core refractive index (Rayleigh scattering), scattering due to irregularities at the boundary between core and cladding, bending loss, loss at joints and connectors and the coupling losses at the input and output.

Remarkable progress has been made in reducing the transmission loss, which is about two orders of magnitude lower than that of coaxial cables having a similar transmission bandwidth. The absorption loss at some wavelengths is almost negligible and below about $0.8\mu\text{m}$ scattering is the dominant factor.

The main cause of absorption is the presence of transition metals such as Fe, Cu (especially in multicomponent glasses), water in the form of OH^- ions and the intrinsic absorption of the pure glass itself. In order to reduce the absorption to an acceptable level, it is necessary to prevent a metal concentration of more than 1 in 10^9 , and an OH radical concentration of more than 1 in 10^7 , from occurring.

6

Another purely material effect is the scattering due to inhomogeneities in the refractive index. These fluctuations are on a scale which is smaller than the wavelength and the resulting Rayleigh scattering is inversely proportional to the fourth power of the wavelength (λ^{-4}), so that it becomes rapidly smaller at longer wavelengths.

The transmission of a single-mode fibre is shown in Figure 1 and exhibits the characteristic features of fibres made by the modified CVD process. In this particular case the core diameter is $10.5\mu\text{m}$, the relative refractive-index difference is $\Delta = 0.17\%$ and the cut-off wavelength of the second set of modes (TM_{01} , TE_{01} and HE_{21}) is $1.2\mu\text{m}$. At short wavelengths the attenuation is inversely proportional to the fourth power of the wavelength and therefore confirms Rayleigh scattering.

The rise in attenuation beyond $1.7\mu\text{m}$ is attributed to the intrinsic infra-red absorption of the glass. The effect of OH^- impurities can be clearly seen but are at a much lower level than is normally observed. The fundamental vibration is at $\lambda = 2.8\mu\text{m}$ in silica and there are overtones at $1.39\mu\text{m}$ and $1.24\mu\text{m}$.

The transmission loss at $1.3\mu\text{m}$ is below 0.4dB/km and is 0.16dB/km at $1.55\mu\text{m}$. See also [Miya et al 1979].

A mode conversion loss, and a loss due to radiation, occur if the fibre has small irregularities at the boundary between the core and cladding. However, this interface scattering, which is referred to as "microbending", can be reduced by increasing both

a radius and the index gradient in the core in order to
 a the light intensity at the core/cladding boundary.

ids can also cause mode conversion to occur in addition to
 ygy loss due to radiation.

Propagation in Single-Mode Fibres

analysis of optical fibres follows the same procedure as
 any other transmission line which guides electromagnetic
 Thus solutions of Maxwell's equations and the
 nding wave equation are sought in terms of the appropriate
 equations, using well-established techniques. For each
 ropagating modes it is possible to deduce the spatial
 tion of the electric and magnetic fields, the propagation
 , phase and group velocities, and so on, in the normal
 tical fibres differ in degree only, and not in principle,
 y, hollow metal waveguides, in that they are designed for
 n at frequencies higher by a factor of 10^4 and the guiding
 a is fabricated entirely from dielectric materials since
 re very lossy at optical frequencies.

ic Concepts

electric waveguide supports a finite number of guided
 an infinite number of radiation modes which together
 mplete orthogonal set. Only guided modes are considered

cladding may
 simply
 for the
 . In
 ver is
 ighly seven

licated, but
 act that, in
 ing
 ed in this
 [Gloge 1971]

s of the
 ctively.
 osition of
 on to
 nerate and as

oximation

(3)

pace wave
 e index and
 on constant β
 $k < \beta < n_1 k$.

The fibre is circular in cross-section and the solutions of the
 wave equation are separable, having the form:

$$\psi = E(r) \cos \nu \theta \exp [j(\omega t - \beta z)] \quad (4)$$

For simplicity the factor $\exp[j(\omega t - \beta z)]$ will be omitted from later
 equations.

In single-mode fibres only the fundamental LP_{01} mode
 propagates and it has no azimuthal dependence, i.e. $\nu = 0$. It
 corresponds to the HE_{11} mode derived from the exact analysis. For
 this fundamental mode equation (3) reduces to

$$\frac{d^2 E}{dr^2} + \frac{1}{r} \frac{dE}{dr} + [n^2(r)k^2 - \beta^2]E = 0 \quad (5)$$

In a step-index fibre, i.e. one with a constant refractive index
 n_1 in the core, equation (5) is Bessel's differential equation and
 the solutions are cylinder functions. The field must be finite at
 $r = 0$ and therefore in the core region the solution is a Bessel
 function J_ν . Similarly the field must vanish as $r \rightarrow \infty$ so that the
 solution in the cladding is a modified Bessel function K_ν . For
 the fundamental LP_{01} mode polarised in either the x or y direction
 the field is therefore [Snyder 1969A]

$$\begin{aligned} E(r) &= AJ_0(UR) \quad R < 1 \text{ (core)} \\ &= AJ_0(U) \frac{K_0(WR)}{K_0(W)} \quad R > 1 \text{ (cladding)} \end{aligned} \quad (6)$$

where $R = r/a$ is the normalised radial coordinate and A is the amplitude coefficient. U and W are the eigenvalues in the core, and cladding, respectively, and are defined by

$$U^2 = a^2(n_1^2 k^2 - \beta^2) \quad (7)$$

$$W^2 = a^2(\beta^2 - n_2^2 k^2)$$

therefore

$$V^2 = a^2 k^2 (n_1^2 - n_2^2) = U^2 + W^2$$

Related to these parameters is the normalised propagation constant b , defined as [Gloge 1971]

$$b = [(\beta/k)^2 - n_2^2] / 2n_1^2 \Delta = 1 - \frac{U^2}{V^2} \quad (8)$$

where

$$\Delta = \frac{n_1^2 - n_2^2}{2n_1^2} = \frac{n_1 - n_2}{n_1} \leq 1$$

Since, for a guided mode, the limits of β are $n_2 k$ and $n_1 k$ then b must lie between 0 and 1.

The field expressions in equation (6) are normalised so as to have the same value at $r = a$. In addition the tangential electric field components must be continuous at this point, leading to the following eigenvalue equation for the LP_{01} mode:

$$\frac{U J_1(U)}{J_0(U)} + \frac{W K_1(W)}{K_0(W)} \quad (9)$$

It should be noted that it is only because of the weak-guidance approximation that the boundary conditions of the magnetic field components are also satisfied by this condition.

By solving equations (7) and (9) the eigenvalue U , and hence β , can be calculated as a function of the normalised frequency V . Therefore the dependence of the propagation characteristics of the mode on the wavelength and fibre parameters can be determined.

At the lower limit of $\beta = n_2 k$ the mode phase velocity equals the velocity of light in the cladding and the wave is no longer guided, the mode is cut off and the eigenvalue $W = 0$ (equation (7)). As β increases, less power is carried in the cladding and at $\beta = n_1 k$ all the power is confined to the core.

The limit of single-mode operation is determined by the wavelength at which the propagation constant of the second LP_{11} mode equals $n_2 k$. For a step-index fibre this cut-off condition is given by

$$J_0(V_C) = 0$$

where V_C denotes the cut-off value of V which, for the LP_{11} mode, is equal to 2.405. The fundamental mode has no cut-off, hence single-mode operation is possible for $0 \leq V \leq 2.4$.

4. Dispersion in Single-Mode Fibres

The bandwidth of optical fibres is limited by broadening of the propagating light pulse which has a finite spectral width due to (i) the spectral width of the source, and (ii) the modulation sidebands of the signal. If, therefore, the fibre waveguide is dispersive the different frequency components will travel at different velocities resulting in pulse distortion.

The transit time for a light pulse propagating along a fibre of length L is

$$\tau = \frac{L}{c} \frac{dB}{dk} \quad (10)$$

where c is the velocity of light.

If B varies non-linearly with wavelength the fibre will be dispersive. From equation (8) we have

$$B^2 = k^2 n_1^2 [1 - 2A(1 - b)] \quad (11)$$

Thus B is a function of the refractive indices of the core and cladding materials and of b . Equation (8) shows that b is a function of V so that pulse dispersion arises from the variation of b with the ratio a/λ . In addition, the refractive index of the fibre material varies non-linearly with wavelength and this also gives rise to pulse dispersion.

The pulse spreading caused by dispersion is given by the derivative of the group delay with respect to wavelength [Payne & Gambling 1979]

$$\text{pulse spread} = \left| \delta\lambda \frac{d\tau}{d\lambda} \right| L = \frac{L}{c} \frac{2\pi}{\lambda^2} \frac{dB}{dk^2} \delta\lambda \quad (12)$$

where $\delta\lambda$ is the spectral width of the source. Substituting equation (11) into equation (12), and differentiating with respect to k , gives the dependence of the pulse spreading on the material properties and the mode parameter b . The dependence on the refractive index is given in terms of the material dispersion parameter $-(1/c)(d^2n/d\lambda^2)$ where $n = n_1$ or n_2 and the dependence on b is given by the mode dispersion parameter defined as $V(d^2(bV)/dV^2)$. In addition, a third term, which is proportional to $dA/d\lambda$, arises from the differentiation in equation (12).

The preceding three effects are inter-related in a complicated manner, but [Gambling, Matsumura & Ragdale 1979A] show that the expression for pulse spreading can be separated into three composite dispersion components in such a way that one of the effects dominates each term. For example, a composite material dispersion term can be defined which has a dependence on both b and $d^2n/d\lambda^2$, however it becomes zero when $d^2n/d\lambda^2$ is zero.

In multimode fibres the majority of the modes are far from cut off and most of the power is carried in the core. In this case the composite dispersion components simplify to terms which depend on either material or mode dispersion, and the two effects can be separated. In addition, in step-index multimode fibres the effect of $dA/d\lambda$ can be neglected.

Material and mode dispersion also have a dominant effect in single-mode fibres but the effect of $d\Delta/d\lambda$ can no longer be neglected [Gambling, Matsumura & Ragdale 1979A].

In the absence of material dispersion the pulse spreading is controlled by the mode parameter $Vd^2(bV)dV^2$ which is shown in Figure 2(a) as a function of V for the LP_{01} mode. In the single-mode regime, i.e. $V < 2.4$, the mode dispersion is always positive and reaches a maximum at $V = 1.15$. It is seen that a change in any of the waveguide parameters, e.g. core radius or wavelength, changes V and hence the mode dispersion.

The material dispersion parameter, $(\lambda/c)(d^2n/d\lambda^2)$ is plotted as a function of wavelength in Figure 2(b) for a germanophospho-silicate glass fibre with $NA = 0.2$. At most wavelengths the material dispersion exceeds mode dispersion, but at $1.29\mu\text{m}$ the material dispersion is zero [Payne & Gambling 1975] (i.e. $dr/d\lambda = 0$). Thus at wavelengths near this value the bandwidth is limited by mode dispersion.

The total dispersion of a single-mode fibre arises from the combined effects of material dispersion, mode dispersion and $d\Delta/d\lambda$ terms. As shown in Figure 2(b) the material dispersion function changes sign at a wavelength of approximately $1.29\mu\text{m}$, whereas mode dispersion always has the same sign in the single-mode regime. Therefore the effects of material dispersion, $d\Delta/d\lambda$ and mode dispersion can be balanced to give zero first-order dispersion at a given wavelength [Gambling, Matsumura & Ragdale 1979A]. Hence

extremely large bandwidths can, in theory and practice, be achieved in single-mode fibres.

Since the dispersive properties of the fibre depend on both the fibre core dimensions and the fibre materials the total dispersion can be altered by changing either of these parameters. The wavelength λ_0 at which the first-order dispersion is zero can therefore be tuned by appropriate choice of the core diameter or of NA . The total dispersion is plotted in Figure 3 as a function of wavelength for different core diameters and a fixed NA of 0.23.

The range of wavelengths over which λ_0 can be tuned is limited. The maximum value depends on the usable value of NA , while the minimum value is approximately the wavelength at which material dispersion is zero ($\sim 1.3\mu\text{m}$).

If a fibre is designed to operate with zero first-order dispersion the limitations imposed on the bandwidth by secondary effects must be considered. For example, birefringence arising from ellipticity or stress in the core causes the two orthogonally-polarised modes of the "single-mode fibres" to become distinguishable, i.e. they are no longer degenerate as in the scalar approximation [Adams et al 1979] [Love et al 1979]. The modes have different propagation constants which results in pulse dispersion. The dispersion caused by a difference between the major and minor axes of about 5% is less than 2 ps/km and can therefore be neglected [Adams et al 1979]. On the other hand the pulse dispersion arising from stress birefringence may be as high as 40ps/km if the expansion coefficients between the fibre core and cladding materials are not matched [Norman et al 1979].

Figure 4 shows the bandwidth of a single-mode fibre designed for $\lambda_0 = 1.3\mu\text{m}$. In the absence of second-order effects the bandwidth is usually limited by the spectral width of the source. Thus the solid line shows the available bandwidth with a source of linewidth 1nm . On the other hand if stress birefringence introduces a pulse dispersion of 10ps/km the bandwidth in the vicinity of λ_0 is considerably reduced (dotted curve). In the absence of polarisation dispersion the bandwidth near λ_0 would be determined by higher-order effects.

Measurements with a narrow-linewidth laser source over a 20km length have revealed a pulse dispersion of less than 4ps/km in a typical fibre.

5. Spot Size

The spot size of the fundamental mode is one of the most important parameters in single-mode fibre design since it largely determines the launching efficiency, jointing loss and bending loss. Usually the spot size w_0 is defined as the width to $1/e$ intensity of the LP_{01} mode or, alternatively, in terms of the spot size of an incident Gaussian beam which gives maximum launching efficiency. The latter definition arises from the fact that the LP_{01} mode has almost a Gaussian distribution.

The spot size is a function of both V and NA , although the dependence on V is only slight [Gambling & Matsumura 1977] (w_0 changes by only 2% over the range $V = 1.8$ to 2.4). The numerical aperture, on the other hand, has a strong effect since a

large NA increases the guidance effect and more of the power in the LP_{01} mode is confined to the core, so that the spot size decreases.

6. Launching Efficiency

The ratio of power accepted by the fibre to the power in an incident beam is defined as the launching efficiency and can be calculated by integrating the product of the incident and propagating modes over the fibre cross-section [Snyder 1969B].

Thus launching efficiency

$$= \frac{1}{\pi I} \left| \int^A E_{\text{inc}} \cdot E \, dA \right|^2 \int^A E_{\text{inc}}^2 dA \int^A E^2 dA \quad (13)$$

where E_{inc} is the electric field distribution of the incident mode.

Maximum power is launched into the fibre when the spot size of the LP_{01} mode is matched to the waist of the incident Gaussian beam. In practice, however, the launching efficiency of the LP_{01} mode decreases if the input beam is offset or tilted.

7. Joint Loss

The efficiency with which power can be coupled between two fibres is determined by the extent to which the mode patterns of the incoming and outgoing fibres can be matched. Therefore angular or lateral misalignment can considerably increase the loss at a joint. While longitudinal separation between the ends of the

fibres can also occur, its effect on loss in practical joints is small enough to be neglected.

If it is assumed that the spot sizes of the modes of the two fibres are the same then the joint loss can be derived simply in terms of spot size. In the absence of angular misalignment the loss caused by lateral offset is [Gambling, Matsumura & Ragdale 1978]

$$T_l = 2.17(D/w_0)^2 \text{dB} \quad (14)$$

where D is the offset. The offset loss is thus inversely proportional to the square of the spot size, w_0 . On the other hand the loss caused by an angular misalignment α is

$$T_a = 2.17 (\alpha w_0 n V / a NA)^2 \text{dB} \quad (15)$$

and hence angular misalignment loss is directly proportional to the square of the spot size. Thus for a given loss there is a trade-off between the spot size, and hence NA , required for low offset loss and that required for low angular misalignment loss.

When angular and lateral misalignments occur together the combined effect is complicated [Gambling, Matsumura & Ragdale 1978], but if the total loss is small it can be approximated by the sum of equations (14) and (15).

8. Bending Loss

Radiation at bends in single-mode fibres can significantly increase the transmission loss [Petermann 1977] [Gambling, Matsumura & Ragdale 1979B]. The bending loss can arise either from curvature of the fibre axis or microbending, i.e. small inhomogeneities in the fibre such as diameter variations, which can arise during coating and cabling.

There are two different mechanisms giving rise to bend loss in single-mode fibres, namely transition loss and pure-bend loss [Gambling, Matsumura & Ragdale 1979B] [Gambling, Matsumura, Ragdale & Sammut 1978]. The transition loss is oscillatory and arises because power is lost by coupling between the fundamental mode and the radiation modes. In other words the power distribution in the HE_{11} mode of the straight fibre is different from that of the corresponding mode in the curved fibre and power is lost at the interface between the two due to this mismatch.

The second mechanism, pure-bend loss, represents a loss of energy from the pure mode of the curved fibre and can be explained as follows. At a bend the phase fronts are no longer parallel and at a sufficiently large distance from the centre of curvature the increased distance between the phase fronts corresponds to a phase velocity greater than c/n_2 . This part of the wave is no longer guided and radiates away from the fibre. As the curvature is increased the radius at which the phase velocity equals the velocity of light decreases, hence more energy is lost. The amount of power radiated depends on the spot size. If the spot

size is reduced the power is more tightly guided in the core and the pure-bend loss decreases.

Both the transition loss and pure bend loss are strongly dependent on the NA (and hence the spot size). It is therefore possible to reduce bending loss to a negligible level by increasing the numerical aperture of the fibre.

9. Arbitrary Profiles

In the discussions above only a stepped refractive-index profile has been considered. In practice, however, the real profiles of single-mode fibres have a dip in the centre and some grading of the core/cladding boundary is caused by diffusion of dopants during the fabrication process. In addition the refractive index in the cladding is not usually constant. The field distribution and propagation characteristics of the LP_{01} mode are thus different quantitatively, although not qualitatively, from those in the step-index fibre. Hence all of the properties discussed above will be different for fibres with different profiles.

There are two ways of dealing with this problem. The first is to use the measured refractive-index profile to produce a numerical solution [Matsumura et al 1980] of the scalar wave equation (equation (3)). The second method involves matching the mode field of the real fibre to that of a fibre with equivalent step-index distribution [Matsumura et al 1980] [Snyder & Sammut 1979]. This simplifies the problem since the analytical expressions for a step-index fibre can be used; however, it is not

very accurate for fibre profiles which depart too far from a stepped distribution.

10. Propagation in Multimode Fibres

10.1 Basic Concepts

Multimode fibres have larger core diameters and numerical apertures than single-mode fibres and, as a result, can be coupled more easily to optical sources. In particular, light-emitting diodes, which are cheaper and more reliable than lasers, can be used to drive multimode fibre links. Moreover jointing and splicing losses are much lower than with single-mode fibres since the dimensions are larger and hence the alignment tolerances are much less stringent. Finally, multimode fibres are less susceptible to microbending losses. However single-mode fibres have far higher bandwidths than those offered by multimode fibres.

Typical multimode fibres have a core diameter of $50\mu\text{m}$, a numerical aperture of 0.2 (i.e. a relative index difference Δ of slightly less than 1%) and an outer diameter of $125\mu\text{m}$. At a wavelength of $0.85\mu\text{m}$ (the emission wavelength of GaAs devices) the corresponding normalised frequency is $V = 37$ and the number of guided modes (approximately $V^2/4$ for graded-core fibres is ~ 340).

In general, therefore, power is launched into a large number of modes having different spatial field distributions, propagation constants, chromatic dispersion and so on. In an ideal fibre,

having properties (e.g. core size, index difference, refractive-index profile) which are independent of distance, then the power launched into a given mode remains in that mode and travels independently of the power launched into other modes. In addition most of the modes are operated far from cut-off and their properties are, therefore, relatively independent of wavelength. This behaviour contrasts with single-mode operation where the mode parameters, such as normalised propagation constant or power confinement factor, vary rapidly with wavelength.

Since the majority of modes operate far from cut-off, and are thus well confined, most of the power carried by multimode fibres travels in the core region. The properties of the cladding therefore only significantly affect those modes which are near cut-off and whose electromagnetic fields extend appreciably beyond the core.

11. Dispersion in Multimode Fibres

The existence of several hundred modes, each having its own propagation constant, causes a form of pulse distortion which does not exist in single-mode fibres, namely intermodal dispersion. The energy of an impulse launched into a multimode fibre is therefore spread over a time interval corresponding to the range of propagation delays of the modes. The number of signal pulses which may be transmitted in a given period, and hence the information-carrying capacity of the fibre, is therefore reduced. Since, in the absence of mode filtering or mode conversion, the pulse spreading increases linearly with fibre length, the bandwidth is inversely proportional to distance. The product of

bandwidth B and distance L is therefore a figure of merit for the information capacity of an optical fibre. The $B \times L$ product for a step-index fibre is typically 20MHz/km. As indicated in the Introduction, a careful choice of the radial variation of the refractive index enables the transit-times of the modes to be almost equalised so that $B \times L$ products of 10-20GHz/km have been predicted but cannot be achieved in practice. The power-law, or α , class of refractive-index profiles, given by

$$\begin{aligned} n^2(r) &= n_1^2 \left[1 - 2\Delta \left(\frac{r}{a} \right)^\alpha \right] & r < a \\ n^2(r) &= n_1^2 [1 - 2\Delta] = n_2^2 & r > a \end{aligned} \quad (16)$$

has been used extensively to model the grading function of multimode fibres. The profile is optimised by a suitable choice of α . It may be shown [Gloge & Marcattili 1973] [Olshansky & Keck 1976] that, neglecting the dispersive properties of the glasses forming the waveguide, the value of α which minimises the r.m.s. pulse broadening is given by

$$\alpha_{\text{opt}} = 2 - \frac{12\Delta}{5} \quad (17)$$

and the r.m.s. output pulse width produced by a unit impulse at the input is then

$$\sigma_{\text{opt}} = \frac{L}{c} \frac{n_1}{20/3} \Delta^2 \quad (18)$$

The intermodal dispersion is, however, an extremely sensitive function of the index-profile. Minute departures of refractive index from the power law, or an incorrect design of the profile, lead to a much lower bandwidth than is theoretically achievable. For example, an error in α of $\sim 1\%$ degrades the bandwidth by a factor of two. The central dip caused by dopant evaporation in the high-temperature collapse stage of the CVD process, and the step-like structure caused by the deposition of individual glass layers, have been shown to contribute significantly to the pulse broadening.

11.1 Effect of the Wavelength Dependence of Refractive Index

The variation of refractive index with wavelength also causes the transmitted pulses to broaden, as we have seen in the case of single-mode fibres. With multimode fibres an additional, more subtle, effect exists since the index dispersion $dn/d\lambda$ also alters the relative transit-times of the modes and hence, the intermodal dispersion [Olshansky & Keck 1976]. This is normally referred to as "profile dispersion" and is a result of the difference which exists between the group index $N = n - \lambda(dn/d\lambda)$ (which determines the pulse transit time) and the refractive index n .

Since $dn/d\lambda$ is, in general, a function of glass composition it varies across the core of a graded-index fibre. Hence each mode is affected differently by dispersion since the spatial distribution of power is not the same for all modes. For example, low-order modes travel, on average, in a medium of higher dopant concentration than do higher-order modes. Thus a correction to the optimum profile parameter is required.

11.2 Material Dispersion in Multimode Fibres

The power carried by multimode fibres travels almost entirely in the core region. Because, in addition, most modes are operated far from cut-off they are almost free of waveguide dispersion. The pulse delay in multimode fibres is thus given, to first order, by [Gloge 1971]

$$\tau = \frac{L}{c} N_1 = \frac{L}{c} \left(n_1 - \lambda \frac{dn_1}{d\lambda} \right) \quad (19)$$

where N_1 is the group index of the core material. (For graded-index fibres, N_1 represents a value of group index averaged over the core area).

Semiconductor sources used in optical communications systems radiate over a finite range of wavelengths and, from equation (19), each spectral component travels at a different group velocity. The resulting pulse broadening σ_m is known as material dispersion.

For a source of r.m.s. spectral width σ_s and mean wavelength λ_s , σ_m may be evaluated by expanding equation (19) in a Taylor series about λ_s :

$$\sigma_m = \sigma_s \frac{d\tau}{d\lambda} + \frac{\sigma_s^2}{2!} \frac{d^2\tau}{d\lambda^2} + \dots \quad (20)$$

The first term normally dominates, particularly for sources operating in the 0.8 to 0.9 μm wavelength region. Thus for the material illustrated in Figure 2(b) the material dispersion parameter $M = (1/L) (d\tau/d\lambda)$ is $\sim 100\text{ps nm}^{-1}\text{ km}^{-1}$ at 0.85 μm . For a typical light-emitting diode having $\sigma_s = 18\text{nm}$ and $\lambda_s = 850\text{nm}$ the resulting pulse broadening is 1.8ns/km^{-1} which limits the BxL product to 100MHz/km . This level of dispersion is an order of magnitude greater than the intermodal dispersion. Even with semiconductor lasers (having spectral widths of, typically, 1nm r.m.s.) material dispersion sets an ultimate limit on the capacity of multimode fibre systems.

Figure 2(b) shows that a wavelength region exists where the material dispersion parameter is negligible. The wavelength λ_m of zero material dispersion is found to vary according to the glass composition [Payne & Hartog 1977], but for silica-based fibres, is always in the vicinity of 1.3 μm . Operation in this wavelength region substantially reduces the bandwidth limitations arising from material dispersion and greater BxL products are available, even with light-emitting diodes. It may be seen from Figure 1 that, for silica-based glasses, the fibre attenuation is also extremely low (0.38dB/km^{-1}).

As shown in Figure 5, the bandwidth available from multimode fibres increases rapidly as the wavelength of operation is increased from 0.85 μm (emission of GaAlAs devices) to the region of negligible material dispersion ($\sim 1.3\mu\text{m}$). Thus for a laser having a spectral width of 1nm r.m.s. (dashed curve), the information-carrying capacity is limited in the region of 1.3 μm , by residual intermodal dispersion. For a numerical aperture of

0.2 the maximum available bandwidth is $\sim 13\text{GHz/km}$, providing the refractive-index profile is correctly designed.

Material dispersion does not completely vanish, however, even at the wavelength where the first derivative of group delay $d\tau/d\lambda$ is zero. According to equation (22) higher-order terms must then be taken into account [Kapron 1977]. The pulse broadening resulting from second-order material dispersion is proportional to the square of the source linewidth, and for silica-based fibres is of the order of $0.1\text{ps/nm}^2\text{ km}^{-1}$. With laser sources second-order material dispersion is not a serious limitation.

The linewidth of light-emitting diodes increases as the square of the operation wavelength [Gloge et al 1980] and, at 1.3 μm , values of 100nm f.w.h.m. (42nm r.m.s. spectral width) have been reported. With such broad spectral widths, second-order material dispersion limits the bandwidth [Adams et al 1978] to about 2GHz/km^{-1} , see Figure 5, solid curve. Although the bandwidth of the best multimode fibres can, in principle, be limited in this way, in practice a counteractive effect, namely wavelength filtering, takes place. The latter effect results from even minor variations in the loss/wavelength characteristic of the fibre, which are enhanced by transmission over long distances (e.g. 20-30km for typical 1.3 μm systems). Thus, the effective wavelength spread is dictated more by the attenuation characteristics of the fibre than by the spectral width of the source. In addition the wavelength at which the received power is a maximum may not coincide with the peak source wavelength.

12. New Fibres

As indicated in the earlier sections of this chapter, optical fibres have been developed to a high degree of sophistication for applications in long-distance transmission. Silica-based fibres have attenuations close to the theoretical minimum at wavelengths of $0.85\mu\text{m}$, $1.3\mu\text{m}$ and $1.55\mu\text{m}$, while the bandwidth of single-mode fibres can, for all practical purposes, be made almost infinite at wavelengths greater than $1.3\mu\text{m}$. Attention is now being given to the design of new types of fibre for application as active and passive fibre components, as sensors and in other new types of optical circuit element.

At Southampton we have been studying four types of structure, involving new materials and new fibre designs. Firstly we have fabricated fibres with zero birefringence [Barlow et al 1981], strong linear birefringence [Birch et al 1982] and strong circular birefringence [Varnham et al 1985] [Hussey et al 1986]. Secondly, we have made fibres with longitudinal metal components close to the core [Li ?] so that the effect of transverse electric fields can be investigated with a view of producing electrically-activated modulation and switching. Thirdly, a technique has been developed for doping the core of single-mode fibres with rare-earth and transition-metal materials through an extension of the MCVD technique [Poole et al 1985]. Fourthly, we are looking at the fabrication of fibres with non-silica glasses chosen so as to enhance the Kerr, Faraday and acousto-optical effects.

The remainder of the chapter describes some examples of these fibres.

13. Linearly-Birefringent Fibres

In many applications it is necessary that the state of polarisation of the modes in a fibre must be strictly controlled. For example, it is necessary to control linear polarisation in fibres for interferometric sensors, in coherent transmission and for coupling to integrated optical circuits. The state of polarisation in ordinary single-mode fibres is indeterminate. In theory, if a fibre is perfectly constructed so that it is circularly symmetric and laid in a straight line then linearly-polarised light launched at the input will maintain this state along the whole length of the fibre to the output. In practice, however, this does not happen. Firstly, fibres cannot be made as perfect cylindrical structures so that both intrinsic imperfections, as well as external factors such as bends, stress and changes of temperature, produce some optical azimuthal inhomogeneity. Thus linearly-polarised input light may be decomposed into linearly-polarised, orthogonal, components along the two principal transverse planes and these components have different phase velocities. Coupling between the two orthogonal components will cause the state of polarisation to vary along the length of the fibre in an unpredictable way.

In order to stabilise the linear polarisation state it is necessary to reduce the amount of coupling between the two mode components and this can be done by introducing strong linear birefringence into the fibre.

One method of doing so [Dyott et al 1979] is to make the core non-circular in shape so that the refractive-index distributions in the two principal directions are different. Some linearly-birefringent fibres have been made in this way but the refractive-index difference between core and cladding must be large, which means in turn that in order to maintain single-mode propagation the core diameter must be very small. This gives rise to problems of fabrication and jointing of the fibre.

On the other hand, coupling to the non-circular active emission spot of a semiconductor laser is eased and a simple butt connection to a laser diode can have a loss [Dyott] of only 1.9dB. The transmission loss of this type of fibre has been reduced to 9dB/km at 0.85 μ m and 2.5dB/km at 1.3 μ m.

A more common method of producing linear birefringence is by introducing asymmetric stress over the core of the fibre. The core and cladding remain circular, but non-circularly symmetric. sectors of very different expansion coefficient are introduced into the substrate region of the fibre. Several methods have been suggested [Payne, 1984] but the one producing the largest birefringence is the "Bow-Tie" structure [Varnham, Payne, Barlow & Birch 1983] in which the shape of the stress-producing sectors has been optimised to produce the maximum degree of birefringence.

The fibres are fabricated by a modification of the MCVD process [Gambling, Hartog & Ragdale 1981]. After the normal buffer layer has been deposited on the inside of the deposition tube to prevent the diffusion of water into the core and cladding regions, a layer of stress-producing material (for example

borosilicate glass) is deposited. The tube rotation is then stopped and some of the stress-producing glass is etched away on opposite sides of the preform tube. The tube is again rotated and layers of cladding, followed by core, glass are deposited in the usual way. The deposited tube is then collapsed into a solid rod preform. During the collapse process the cusp-like regions of stress-producing glass in the tube assume the "Bow-Tie" shape in the fibre. It is possible to produce a high degree of stress in the preform, even up to the breakdown level of glass thus causing the preform to shatter. Assuming that shattering has not occurred the preform rod is then drawn into a fibre. During the cooling from the drawing temperature of approximately 2000°C to room temperature a high degree of asymmetric stress is once again introduced, due to the different thermal expansion coefficients of the borosilicate sectors and the silica substrate. The fibre, as distinct from the preform, is mechanically strong and is no more likely to break than a conventional fibre.

The degree of birefringence can be easily assessed by observing the light scattered sideways from the fibre. The two propagating polarisation modes run into, and out of, phase at a rate depending on the birefringence, so that the scattered light varies periodically in intensity. Beat lengths of less than 1mm (modal birefringence $B = 6 \times 10^{-4}$) can be obtained. The cross-section of a Bow-Tie fibre is shown in Figure 6. The transmission loss is comparable with that of a normal telecommunications fibre.

14. Polarisation-Maintaining Fibres and Polarising Fibres

As indicated above, the polarisation state in a normal telecommunications fibre is indeterminate. On the other hand a fibre exhibiting a high degree of linear birefringence can operate in two quite distinct ways. In the first of these the two orthogonal modes have a low transmission loss and propagate with roughly equal attenuation. If an equal amount of light is launched into each of the modes then, because of the different phase constants, the state of polarisation changes periodically along the length of the fibre from linear, to circular, to linear, and so on. On the other hand, if only one of the modes is launched, then providing no mode conversion occurs the light will continue to be linearly polarised along the entire length of the fibre. In the presence of strong external distortion some of the original polarisation couples into the orthogonal mode and continues to propagate in that mode to the output.

Another method of operating a Bow-Tie fibre is to introduce attenuation preferentially into one of the modes. Light launched into the low-loss mode will continue in that mode to the end of the fibre. Any light coupled into the orthogonal, i.e. high-loss, mode is attenuated and the output remains linearly polarised despite the mode coupling. Such a fibre is termed a "polarising" fibre, because for any state of input polarisation, only linearly-polarised light emerges.

One method of introducing a preferential loss into one mode is to wind the fibre into a coil. Because of the different refractive-index distributions in the two principal transverse

planes, the bending loss edges of the two modes are at different wavelengths. This effect is illustrated in Figure 7, showing that there is a wavelength region where the attenuation of the two modes is very different. The steepness of the bending edges, their positions and their separation, can be changed by the fabrication conditions, the radius of bend and by microbends [Varnham, Payne, Birch & Tarbox 1983]. The wavelength region in which polarising action occurs can also be controlled. Extinction ratios of 60dB have been obtained, together with wide wavelength windows.

15. Fibres with Negligible Birefringence and Polarisation Mode Dispersion

Fibres with almost zero internal birefringence can be made by rotating the preform of a conventional fibre about its longitudinal axis [Barlow et al 1981] during fibre drawing. Spinning rates of several thousand revolutions per minute are possible, with the result that any azimuthal inhomogeneities rotate along the length of the fibre with a very short pitch length. Linearly-polarised light is unable to follow this rapid rotation of the birefringence axes with the result that the core appears to be circularly asymmetric as far as the propagating mode is concerned. The inherent linear birefringence, and polarisation mode dispersion, can be reduced to a very low level in this way. External effects, such as bends, pressure, etc., can re-introduce birefringence which is not affected by the spun core, so that spun fibres can be used as sensors. They are particularly useful for measurement of magnetic fields and electric currents by exploiting the Faraday effect. Thus the angle of polarisation is rotated by

an amount proportional to the integral of the magnetic field strength along the length of the fibre.

16. Circularly-Birefringent Fibres

It is also possible to produce fibres exhibiting a high degree of circular birefringence. Such fibres can find application in the monitoring of electric current and magnetic fields and also in the control of polarisation in telecommunications.

Probably the simplest method of producing circular birefringence is by twisting a conventional optical fibre about its longitudinal axis. It is then found that the propagation constants of modes polarised in the left-hand, and right-hand, circular directions are different. However, this method is quite limited since, as the fibre will break at beat lengths shorter than about 10cm. Also, of course, a fibre twisted in this way is difficult to handle experimentally.

A much more effective method is to produce a fibre in which the core does not lie along the longitudinal fibre axis but follows a helical path about it. Such fibres have been developed and fabricated at Southampton [Varnham et al 1986] [Reekie et al 1986] by inserting a normal MCVD preform, containing core and cladding, into a hole drilled off-axis in a silica rod. Whilst the silica rod containing the offset core/cladding preform is drawn into fibre it is rotated about its longitudinal axis. The core of the resulting fibre is in the form of a tight helix with a quite short pitch length. The degree of circular birefringence is

more than an order of magnitude greater than is possible by twisting the fibre and beat lengths down to 5mm (corresponding to a modal birefringence of $B = 1.3 \times 10^{-4}$) and less have been produced.

An interesting consequence of this method of fabrication is that the bend loss of the second, and higher-order, modes is greatly increased compared with that of the fundamental mode, so that the fibre can be operated at high normalised frequencies, e.g. $V = 25$, whilst effectively maintaining single-mode operation. The core diameter can thus be much larger than normal. The use of such fibres for measuring magnetic fields and electric currents is now being investigated.

17. Rare-Earth Doping of Single-Mode Fibres

In order to maintain low transmission losses in the near-infra-red wavelength region it is necessary to reduce all but the essential glass constituents of optical fibres to an absolute minimum. In this way, as is well known, transmission losses have been reduced to a few tenths of a decibel per kilometre. On the other hand, optical fibres also have attractive potential applications as sensors and signal-processing devices if the appropriate fibre properties can be introduced, or enhanced, without appreciably increasing the attenuation at the low-loss wavelengths. In the methods discussed so far in this paper the purity of both core and cladding is maintained and the propagating wave is modulated by externally-applied forces such as mechanical strain, electric field, magnetic field, change of temperature, and so on. Another method of modifying the fibre properties is by

introducing small quantities of suitable materials into the core or cladding.

At Southampton a study has been made of possible techniques for introducing rare-earth ions into the light-guiding regions of the fibre. Possible developments could be

- (i) Fibre lasers and amplifiers.
- (ii) Distributed temperature sensor based on
 - (a) absorption, (b) fluorescence.
- (iii) Increased Verdet constant.
- (iv) Increased Kerr effect and non-linear optical coefficients.

We have devised a method of doping fibres through a modification of the MCVD technique [Poole et al 1985]. One of the major advantages of conventional MCVD fabrication is that it enables the appropriate material halides to be used as starting materials and these can be obtained in very pure form and are liquid at room temperature. The problems to be overcome in extending this technique to the rare-earth halides is that they are solid at room temperature, they have a high melting point and thus a low vapour pressure, and they occur in hydrated form.

The method adopted to overcome these difficulties is illustrated in Figure 8. Prior to deposition, a conventional

silica substrate is modified and the required dopant, for example $\text{NdCl}_3 \cdot 6\text{H}_2\text{O}$ (99.9% pure, MP = 758°C) is introduced into a special dopant chamber which is added at the upstream end. The dopant is dried by heating the chamber under a chlorine atmosphere and, at the same time, the anhydrous crystals are fused to the chamber wall. The inside of the deposition tube is then cleaned to remove any dopant which may have been deposited there during the drying process, following which the cladding glass is deposited in the usual way. During the core deposition the dopant chamber is heated to about 1000°C to produce small quantities of NdCl_3 vapour which is carried downstream by the reactant flow where it is oxidised and incorporated into the core. The temperature for core deposition is kept lower than usual so that the core components are initially unfused. Further drying is carried out by heating in a chlorine atmosphere, after which the core is fused into a clear non-porous layer. Subsequent collapse of the deposited tube into a solid rod preform, and drawing of the preform into fibre, are carried out in the usual way.

Initial results have been very successful. A number of dopants, such as neodymium, erbium, ytterbium, terbium and praseodymium, have been incorporated into fibres, giving absorption bands of very high loss (greater than 3000dB/km) at visible and near-infra-red wavelength, whilst maintaining the characteristic low loss (less than 2dB/km⁻¹) in the region of 1.3μm. Further research is proceeding in the study of doping, and co-doping, with other rare-earth and transition metals. Measurements by optical time-domain reflectometry indicate that the dopant is incorporated uniformly along the length of the fibre. The technique is simple, reproducible and can provide

single-component, or multicomponent, doping of a wide range of materials into the core or cladding of both multimode and single-mode optical fibres. The doping level can be varied over a wide range, up to about 1% by weight, without significantly affecting the low-loss characteristics in the wavelength region 0.95 - 1.4 μ m. Such fibres can produce distributed sensors as well as fibre lasers, amplifiers and active components in optical communication systems.

In a measurement of the sensitivity of a neodymium-doped fibre as a temperature sensor the change of absorption edge was measured to be 2dB/km for a 50°C change in temperature.

18. Fibre Lasers and Amplifiers

An example of the absorption spectrum of a lasing fibre is shown in Figure 9 for a single-mode fibre with 30ppm of neodymium in the core. The high-loss absorption bands and the low-loss transmission region are clearly seen. Figure 10 gives the fluorescence spectra for three rare-earth dopants showing the possibility of lasing and amplifying action in three very interesting wavelength regions. So far lasing action has been produced with neodymium and erbium by the simple expedient of placing mirrors at the ends of the length of fibre. A lasing threshold as low as 100 μ W has been observed with a simple diode laser acting as the pump source. One of the mirrors is dichroic allowing good transmission of pump radiation with a high reflectivity of the laser light. Previously reported neodymium fibre lasers have been pulsed or multimode, exhibiting relaxation oscillations, but we have observed CW operation at a power level

of a few microwatts. A ring fibre laser has also been constructed with a fibre coupler to transfer pump radiation into, and laser radiation out of, the cavity. The output power from one port was 2mW for approximately 20mW of pump power absorbed in the ring and a threshold of a few milliwatts. The slope efficiency of well over 20% is much higher than with conventional neodymium/glass lasers and thermal effects are negligible so that the fibre laser can be operated in the CW mode without cooling.

Tunable [Reekie et al 1986] radiation has been produced in both neodymium and erbium fibre lasers by replacing one of the mirrors by a diffraction grating. In the neodymium fibre the argon ion pump radiation at 514nm was coupled into the fibre through the plane input mirror. Even without the diffraction grating the gain available is sufficiently high that feedback from the bare endface of the fibre produced lasing action at a pump power of 122mW. With the grating in place threshold was at 25mW, corresponding to 10mW of pump power in the fibre. The laser is tunable over most of the neodymium gain curve producing an impressive tuning range of 80nm.

The erbium fibre laser operates at a wavelength of 1.536 μ m where the transmission loss of conventional telecommunication fibres is a minimum. Pumping was at 514nm with an argon ion laser. Despite the fact that an erbium laser is a three-level system the small core diameter of 5 μ m allows saturation of the absorption to be easily achieved with only a few milliwatts of pump power, giving an unprecedented low threshold of about 4mW of absorbed power. The output power was several tens of microwatts.

Tunable operation has been achieved over two ranges of 14nm and 11nm near $1.54\mu\text{m}$, with an absorbed pump power of only 90mW.

In addition to the above results optical amplification with high gain has also been achieved as well as Q-switched operation [Mears et al 1986] at $1.55\mu\text{m}$ giving 60ns pulses of 2W peak output power at a repetition rate of 200Hz.

Even from these early results it is clear that optical fibre lasers can produce efficient solid-state sources of low threshold power which are compatible with optical fibre devices and circuits. The output can be tuned in wavelength and fibre lasers should be cheap compared with conventional ones and have the additional virtues of being completely flexible in design and operation. For example, they can be wound into a tight coil without affecting laser action and there is no need for accurate optical alignment of the active medium nor of the mirrors. The latter can be simply attached directly to the end of a fibre cleaved in the normal way. Fibre lasers can be operated in the single, fundamental, mode giving a well-controlled Gaussian output beam. The threshold powers are small, because of the strong guiding action of the core, so that lasing action should be possible with materials having weak transitions and which perhaps have not yet exhibited laser action by other techniques. Again because of the small core diameter cooling is very effective, allowing CW operation at room temperature. The fabrication process is simple and flexible so that a wide variety of dopants can be incorporated very efficiently and economically.

19. Conclusion

It is clear that a wide variety of new optical fibre materials and structures are possible, giving rise to many different types of application. Whilst optical-fibre components cannot compete with integrated optical circuits in terms of size, they are flexible, comparatively simple to fabricate and are compatible with optical fibre transmission lines, avoiding the large coupling loss between fibres and planar optical circuits. In addition to passive devices such as couplers and filters a wide variety of active components can be devised, ranging from optical amplifiers and tunable sources to devices based on non-linear interactions involving soliton propagation, Raman interaction and the like.

Adams, M.J., Payne, D.N. and Ragdale, C.M.:
Birefringence in optical fibres with elliptical cross section,
Electronics Letters, 14, 1979, pp. 298-299.

Adams, M.J., Payne, D.N., Sladen, F.M.E. and Hartog, A.H.:
Optimum operating wavelength for chromatic equalisation in
multimode optical fibres,
Electronics Letters, 14, 1978, pp. 64-66.

Barlow, A.J., Payne, D.N., Hadley, M.R. and Mansfield, R.J.:
Production of single-mode fibres with negligible intrinsic
birefringence and polarisation mode dispersion,
Electronics Letters, 17, 1981, pp. 725-726.

Birch, R.D., Payne, D.N. and Varnham, M.P.:
Fabrication of polarisation-maintaining fibres using gas-phase
etching,
Electronics Letters, 18, 1982, pp. 1036-1038.

Dyott, R.B.:
Private communication.

Dyott, R.B., Cozens, J.R. and Morris, D.G.:
Preservation of polarisation in optical fibre waveguides with
elliptical cores,
Electronics Letters, 15, 1979, pp. 380-382.

Gambling, W.A., Hartog, A.H. and Ragdale, C.M.:
Optical fibre transmission lines,
The Radio & Electronic Engineer, 51, 1982, pp 313-325.

Gambling, W.A. and Matsumura, H.:
Simple characterisation factor for practical single-mode fibres,
Electronics Letters, 13, 1977, pp. 691-693.

Gambling, W.A., Matsumura, H. and Ragdale, C.M.:
Curvature and microbending losses in single-mode optical fibre,
Optical & Quantum Electronics, 11, 1979B, pp. 43-59.

Gambling, W.A., Matsumura, H. and Ragdale, C.M.:
Joint loss in single-mode fibres,
Electronics Letters, 14, 1978, pp. 491-493.

Gambling W.A., Matsumura, H. and Ragdale, C.M.:
Mode dispersion, material dispersion and profile dispersion in
grade-index single-mode fibres,
IEE J. Microwaves, Optics & Acoustics, 3, 1979A, pp. 239-246.

Gambling, W.A., Matsumura, H., Ragdale, C.M. and Sammut, R.A.:
Measurement of radiation loss in curved single-mode fibres,
IEE J. Microwaves, Optics & Acoustics, 2, 1978, pp. 134-140.

Gloge, D.:
Weakly guiding fibres,
Applied Optics, 10, 1971, pp. 2252-2258.

Gloge, D. and Marcatili, E.A.J.:
Multimode theory of graded-core fibres,
Bell Syst. Tech. J., 52, 1973, pp. 1563-1578.

Gloge, D., Ogawa, K. and Cohen, L.G.:
Baseband characteristics of long-wavelength led systems",
Electronics Letters, 16, 1980, pp. 366-367.

Hussey, C.D., Birch, R.D. and Fujii, Y.:
Circularly-birefringent single-mode optical fibres,
Electronics Letters, 22, 1986, pp. 129-130.

Kapron, F.P.:
Maximum information capacity of fibre-optic waveguides,
Electronics Letters, 13, 1977, pp. 627-629.

Li, L., Birch, R.D. and Payne, D.N.:
High performance composite metal/glass fibre polarisers,
Proc. 12th European Conference on Optical Communication,
Barcelona, 1986, pp. 137-140.

Love, J.D., Sammut, R.A. and Snyder, A.W.:
Birefringence in elliptically deformed optical fibres,
Electronics Letters, 15, 1979, pp. 615-616.

Matsumura, H., Suganuma, T. and Katsuyama, T.:
Simple normalization of single-mode fibres with arbitrary index
profile,
Proc. 6th European Conference on Optical Communication, York,
1980.

Mears, R.J., Reekie, L., Poole, S.B. and Payne, D.N.:
Q-switched fibre laser operating at 1.55 μ m,
Electronics Letters, 22, 1986, pp. 159-160.

Miya, T., Teranuma, Y., Hosaka, T. and Miyashita, T.:
Ultimate low-loss single-mode fibre at 1.55 μ m,
Electronics Letters, 15, 1979, pp. 106-108.

Norman, S.R., Payne, D.N., Adams, M.J. and Smith, A.M.:
Fabrication of single-mode fibres exhibiting extremely low
polarization birefringence,
Electronics Letters, 15, 1979, pp. 309-311.

Olshansky, R. and Keck, D.B.:
Pulse broadening in graded-index optical fibres,
Applied Optics, 15, 1976, pp. 483-491.

Payne, D.N.:
Update on polarisation-maintaining fibres,
Proc. Optical Fibre Communication Technical Digest, New Orleans,
1984, Paper ME2.

Payne, D.N. and Gambling W.A.:

Zero material dispersion in optical fibres,
Electronics Letters, 11, 1975, pp. 176-178.

Payne, D.N. and Hartog, A.H.:

Determination of the wavelength of zero material dispersion in
optical fibres by pulse-delay measurements,
Electronics Letters, 13, 1977, pp. 627-629.

Petermann, K.:

Fundamental mode microbending loss in graded-index and W fibres,
Optical & Quantum Electronics, 9, 1977, pp. 167-179.

Poole, S.B., Payne, D.N. and Petermann, M.E.:

Fabrication of low-loss optical fibres containing rare-earth
ions,
Electronics Letters, 21, 1985, pp. 737.

Rawson, H.:

Inorganic glass-forming systems,
Academic Press, London, 1967, p. 317.

Reekie, L., Mears, R.J., Poole, S.B. and Payne, D.N.:

Tunable single-mode fibre lasers,
Journal of Lightwave Technology, LT-4, 1986, pp. 256-260.

Snyder, A.W.:

Asymptotic expressions for eigenfunctions and eigenvalues of a
dielectric optical waveguide,
IEEE Trans. on Microwave Theory & Techniques, MTT-17, 1969A,
pp. 1130-1138.

Snyder, A.W.:

Excitation and scattering of modes on a dielectric or optical
fiber,
IEEE Trans. on Microwave Theory & Techniques, MTT-17, 1969B,
pp. 1138-1144.

Snyder, A.W. and Sammut, R.A.:

Fundamental (HE₁₁) modes of graded optical fibres,
J. Opt. Soc. Am., 69, 1979, pp. 1663-1671.

Suematsu, Y. and Iga, K.-I.:

Introduction to optical fibre communications,
Translation edited by W.A. Gambling,
John Wiley & Sons, New York 1982, p. 208.

Varnham, M.P., Birch, R.D. and Payne, D.N.:

Helical-core circularly-birefringent fibres,
Proc. 5th European Conference on Optical Communication, Venice,
1985, pp. 135-138.

Varnham, M.P., Birch, R.D., Payne, D.N. and Love, J.D.:

Design of helical-core circularly-birefringent fibres,
Proc. Optical Fibre Communication Technical Digest, Atlanta, 1986,
Paper TUL20.

Varnham, M.P., Payne, D.N., Barlow, A.J. and Birch, R.D.:

Analytic solution for the birefringence produced by thermal stress
in polarisation-maintaining optical fibres,
Journal of Lightwave Technology, LT-1, 1983, pp. 332-339.

47

Varnham, M.P., Payne, D.N., Birch, R.D. and Tarbox, E.J.:
Single-polarisation operation of highly-birefringent bow-tie
optical fibres,
Electronics Letters, 19, 1983, pp. 246-247.

FIGURE CAPTIONS

- Figure 1 Transmission loss of a single-mode fibre with germanosilicate core of $10.5\mu\text{m}$ diameter and phosphosilicate cladding. Peaks due to OH^- are present at 1.24 and $1.39\mu\text{m}$.
- Figure 2 (a) The mode dispersion parameter $V(d^2bV)/dV^2$ as a function of normalised frequency V for the fundamental LP_{01} mode.
(b) The material dispersion parameter, $(-1/c)(d^2n/d\lambda^2)$ as a function of wavelength for a germanosilicate glass fibre with $\text{NA} = 0.2$.
- Figure 3 Total first-order chromatic dispersion of a single-mode fibre for core diameters of 4 , 5 and $6\mu\text{m}$. The numerical aperture is 0.23 in each case.
- Figure 4 Bandwidth of a single-mode fibre designed for $\lambda_0 = 1.3\mu\text{m}$, assuming a source linewidth of 1nm and that second-order effects are small. The dotted curve shows the effect of a polarisation dispersion of 10ps/km .
- Figure 5 Bandwidth limitation resulting from material dispersion in a typical $\text{GeO}_2\text{-P}_2\text{O}_5\text{-SiO}_2$ multimode fibre (see Fig. 4(b) for dispersion data). The dashed curve applies to a semiconductor laser source having a spectral width of 1nm r.m.s. The solid line is for a typical l.e.d. having a spectral width given by $\lambda^2/4 \times 10^4$ nm. For a numerical aperture of 0.2 ($\Delta \approx 1\%$), residual intermodal dispersion alone limits the $B \times L$ product to the value shown by the dotted line.
- Figure 6 Cross-section of Bow-Tie fibre showing central core and cladding regions and (dark) stress-producing sectors.
- Figure 7. Transmission loss of the two orthogonally-polarised modes in a Bow-Tie fibre.
- Figure 8 Modified deposition tube for rare-earth doping.
- Figure 9 Absorption spectrum of neodymium fibre laser.
- Figure 10 Fluorescence spectra for fibres doped with terbium, neodymium and erbium.

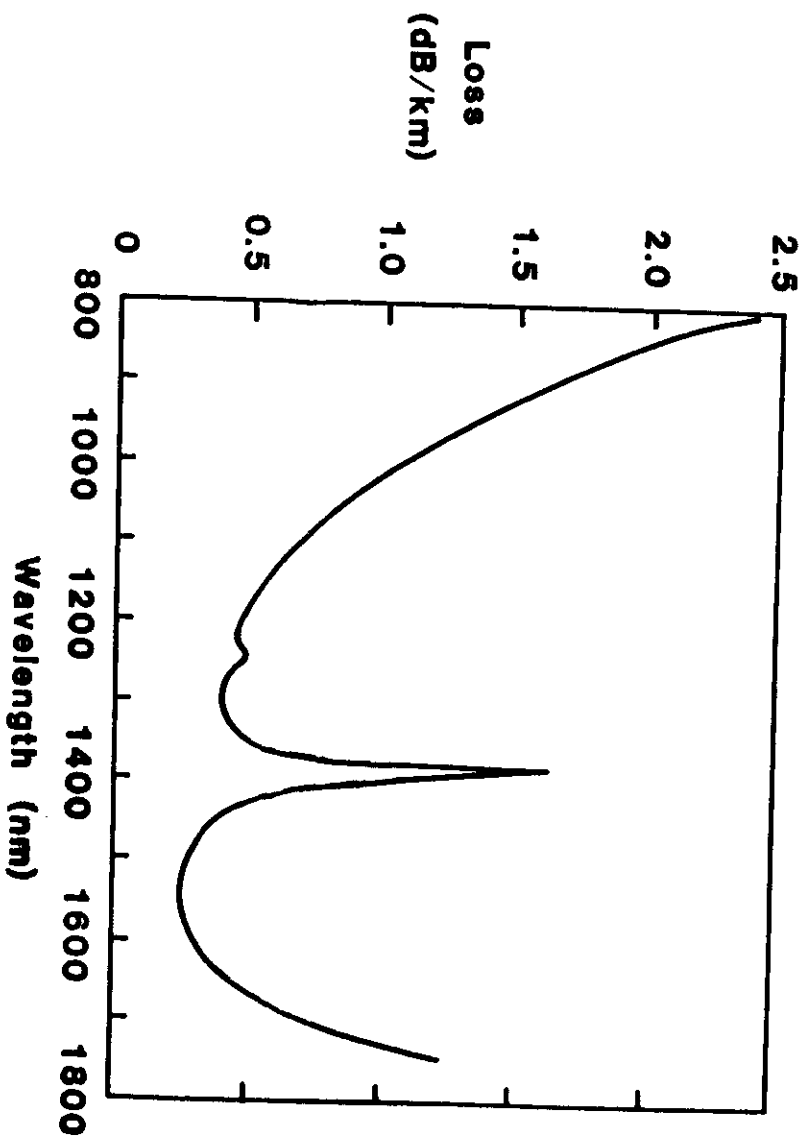
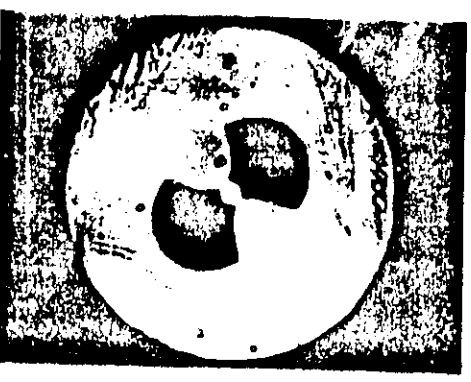
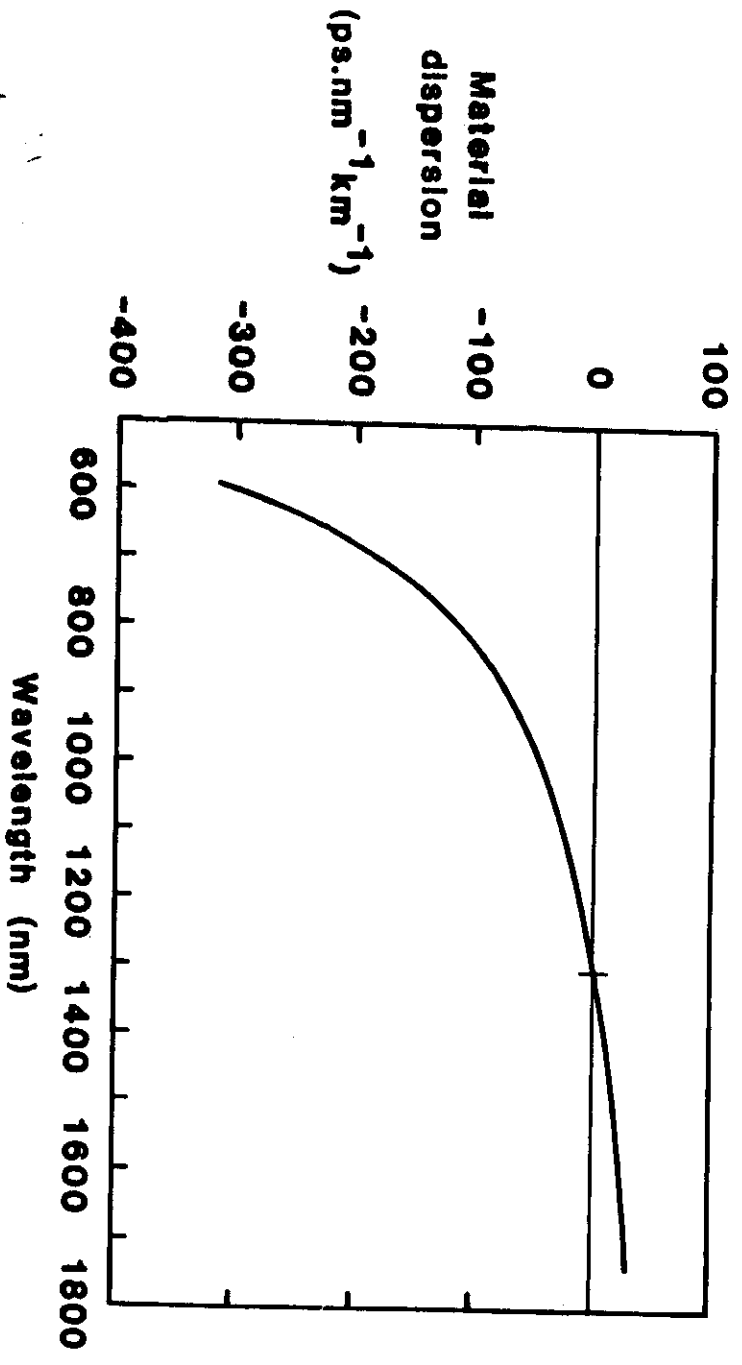


Figure 1

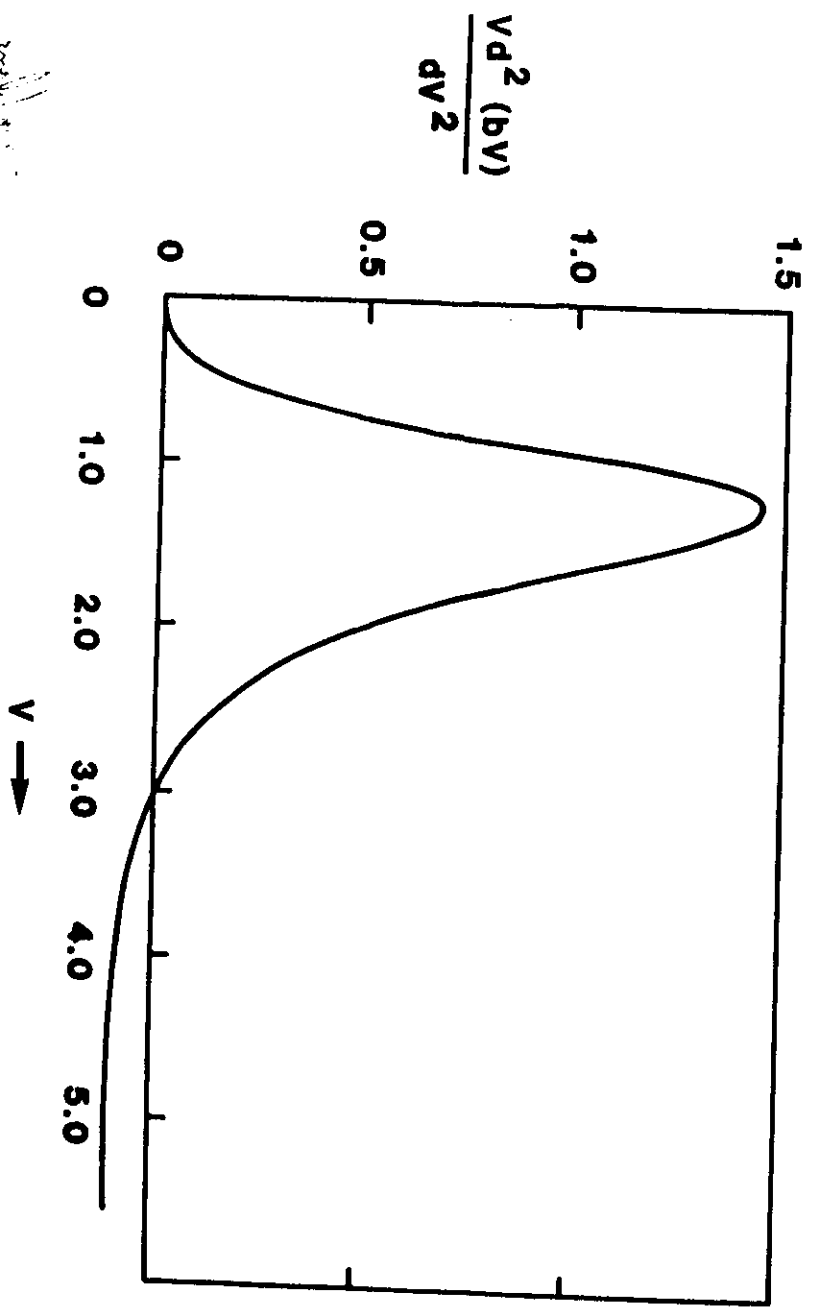
47



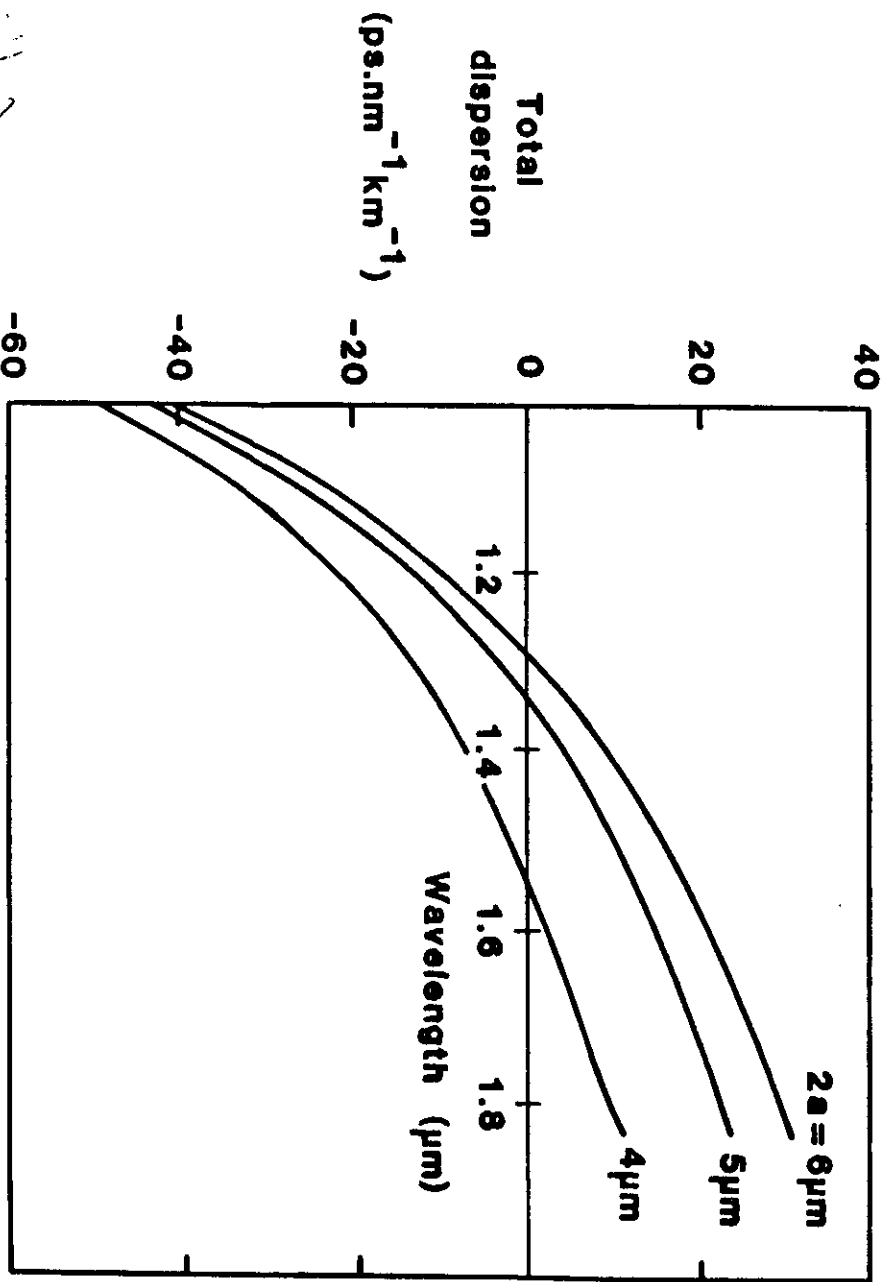
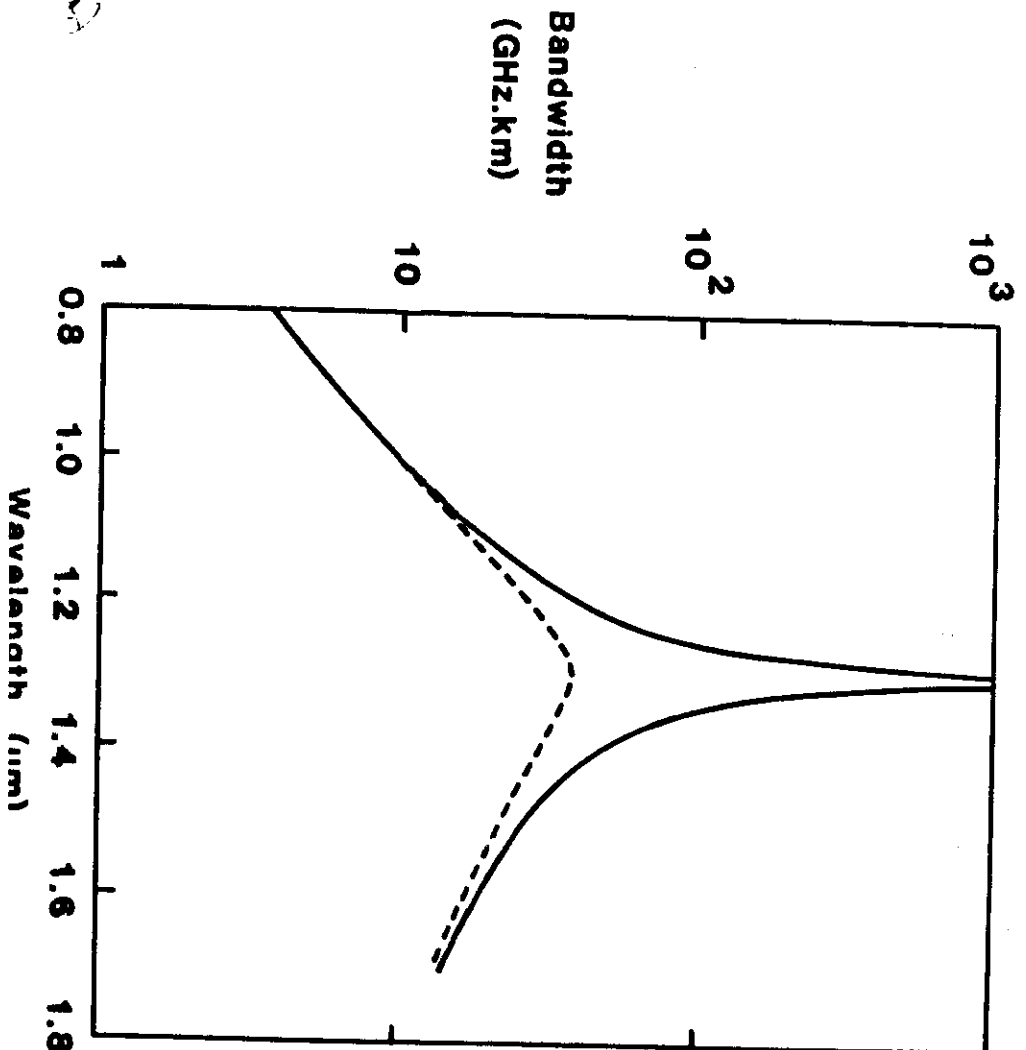


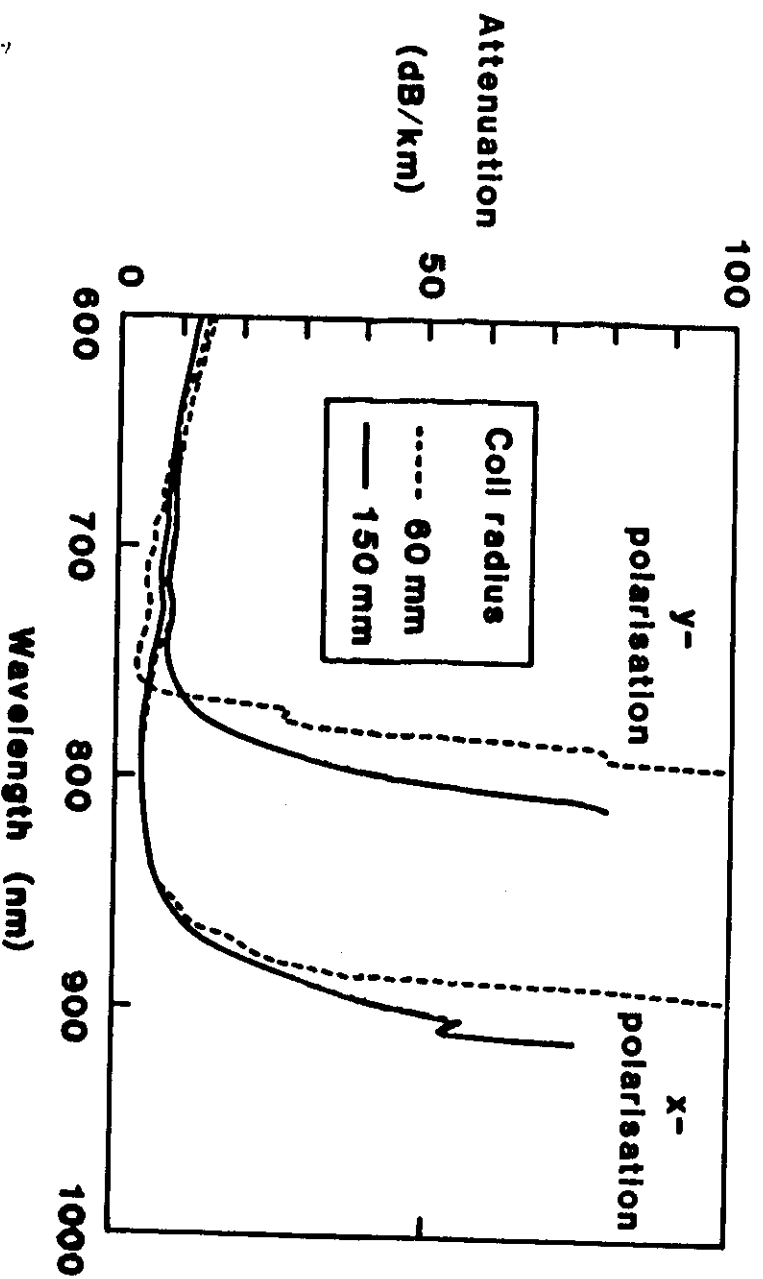
Example 1

15

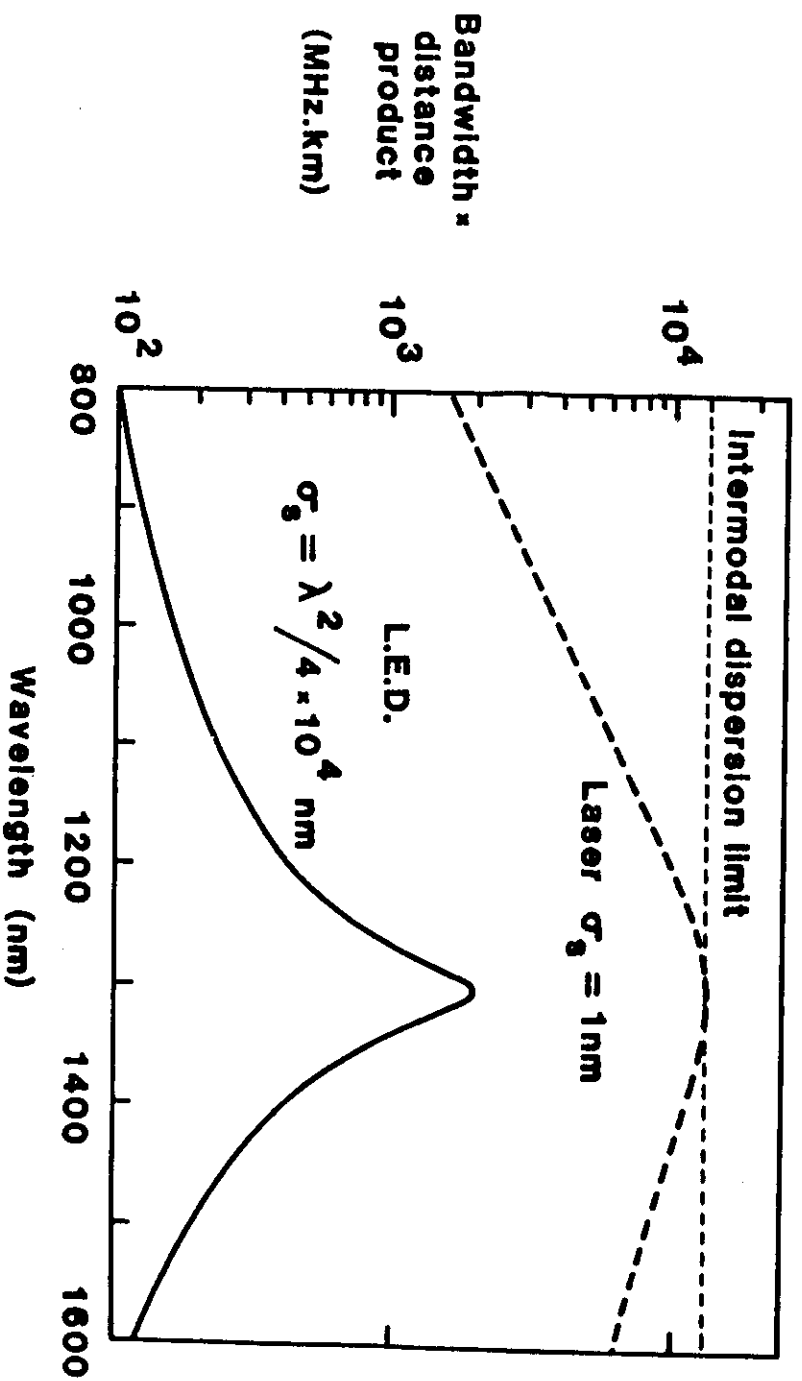


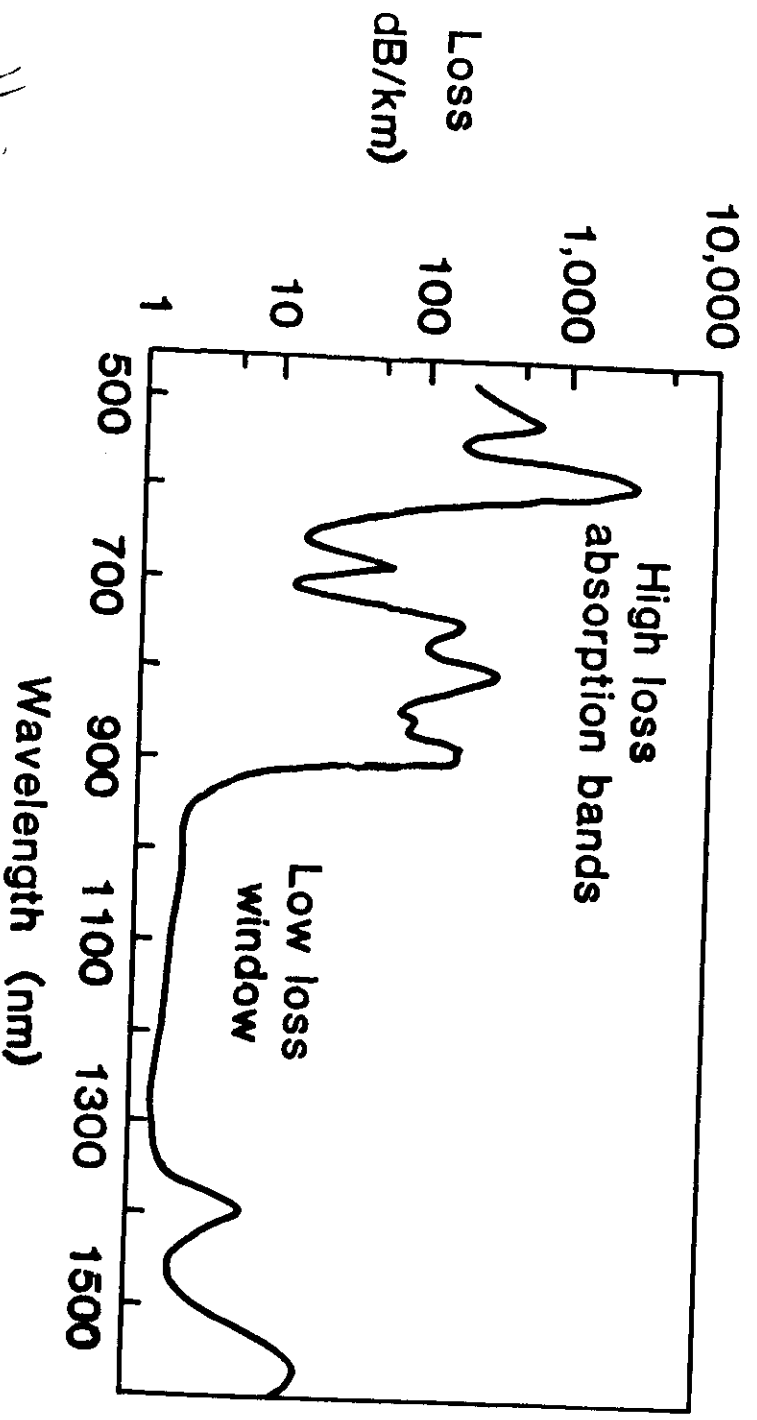
Example 2



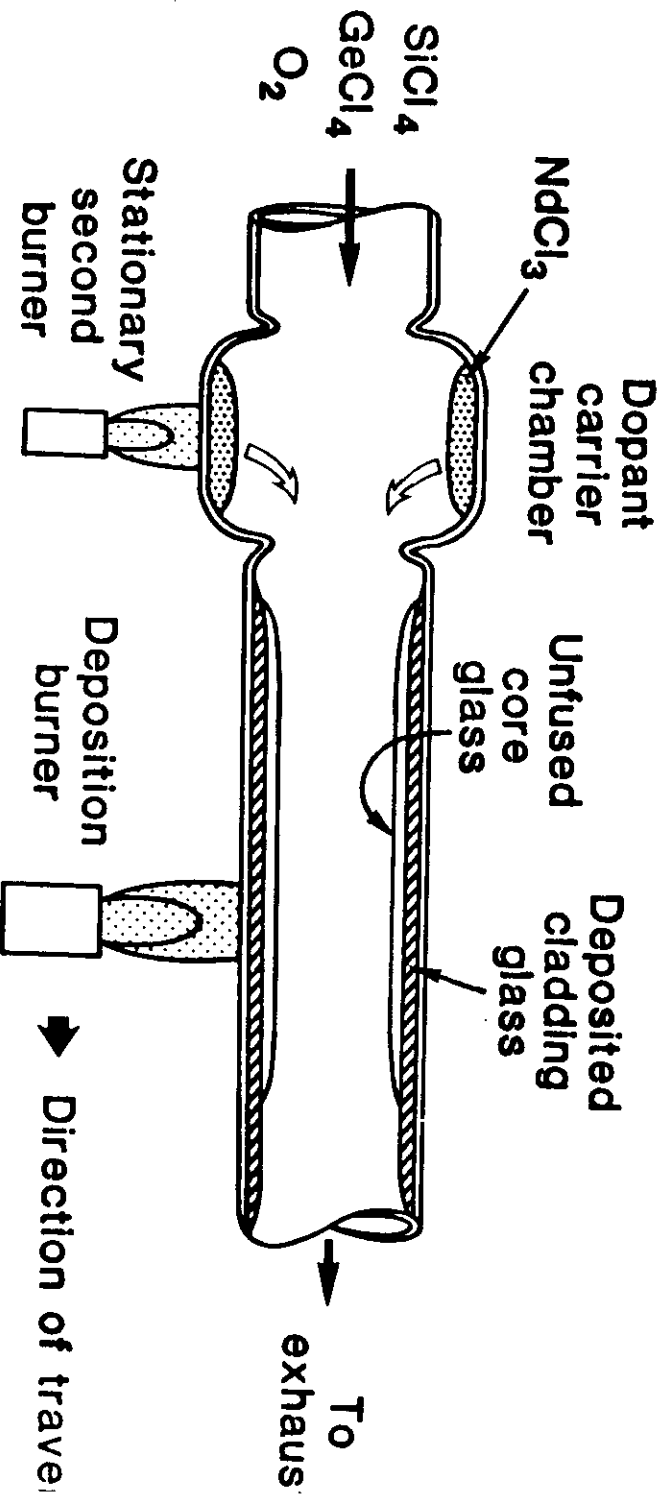


52



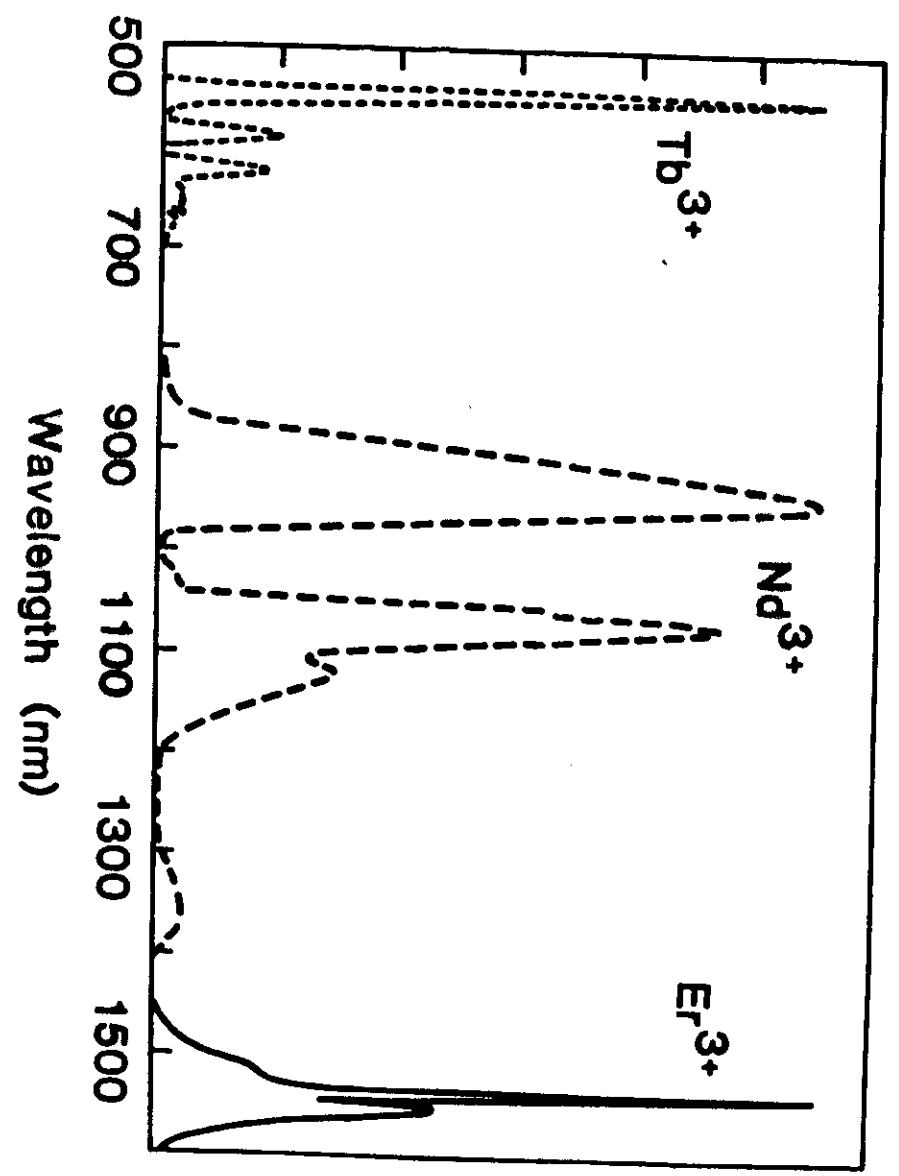


Handwritten signature



Handwritten signature

Fluorescence
(arbitrary
units)



Er³⁺
Nd³⁺
Tb³⁺

Er³⁺
Nd³⁺
Tb³⁺

